

THE OFFICIAL MAGAZINE OF THE OCEANOGRAPHY SOCIETY

Oceanography

CITATION

Wilcock, W.S.D., R.P. Dziak, M. Tolstoy, W.W. Chadwick Jr., S.L. Nooner, D.R. Bohnenstiehl, J. Caplan-Auerbach, F. Waldhauser, A.F. Arnulf, C. Baillard, T.-K. Lau, J.H. Haxel, Y.J. Tan, C. Garcia, S. Levy, and M.E. Mann. 2018. The recent volcanic history of Axial Seamount: Geophysical insights into past eruption dynamics with an eye toward enhanced observations of future eruptions. *Oceanography* 31(1):114–123, <https://doi.org/10.5670/oceanog.2018.117>.

DOI

<https://doi.org/10.5670/oceanog.2018.117>

COPYRIGHT

This article has been published in *Oceanography*, Volume 31, Number 1, a quarterly journal of The Oceanography Society. Copyright 2018 by The Oceanography Society. All rights reserved.

USAGE

Permission is granted to copy this article for use in teaching and research. Republication, systematic reproduction, or collective redistribution of any portion of this article by photocopy machine, reposting, or other means is permitted only with the approval of The Oceanography Society. Send all correspondence to: info@tos.org or The Oceanography Society, PO Box 1931, Rockville, MD 20849-1931, USA.

THE RECENT VOLCANIC HISTORY OF AXIAL SEAMOUNT

Geophysical Insights into Past Eruption Dynamics with an Eye Toward Enhanced Observations of Future Eruptions

By William S.D. Wilcock, Robert P. Dziak, Maya Tolstoy, William W. Chadwick Jr., Scott L. Nooner, DelWayne R. Bohnenstiehl, Jacqueline Caplan-Auerbach, Felix Waldhauser, Adrien F. Arnulf, Christian Baillard, Tai-Kwan Lau, Joseph H. Haxel, Yen Joe Tan, Charles Garcia, Samuel Levy, and M. Everett Mann

- AUTONOMOUS OBS
- MOORED HYDROPHONE
- HYDROTHERMAL MOORING
- ACOUSTIC TRANSPONDER
- AUV WITH DOCKING STATION
- PRIMARY NODE 3B
- CABLED GEOPHYSICAL INSTR.



“ The 2015 eruption at Axial Seamount was the first to be recorded by an in situ cabled observatory, and Axial is now the best-monitored submarine volcano on Earth. ”

ABSTRACT. To understand the processes that form oceanic crust as well as the role of submarine volcanoes in exchanging heat and chemicals with the ocean and in supporting chemosynthetic biological communities, it is essential to study underwater eruptions. The world’s most advanced underwater volcano observatory—the Ocean Observatories Initiative Cabled Array at Axial Seamount—builds upon ~30 years of sustained geophysical monitoring at this site with autonomous and remote systems. In April 2015, only months after the Cabled Array’s installation, it recorded an eruption at Axial Seamount, adding to the records of two prior eruptions in 1998 and 2011. Between eruptions, magma recharge is focused beneath the southeast part of the summit caldera, leading to steady inflation and increasing rates of seismicity. During each eruption, the volcano deflates over days to weeks, coincident with high levels of seismicity as a dike is emplaced along one of the volcano’s rifts and lava erupts on the seafloor. Cabled Array seismic data show that motions on an outward-dipping ring fault beneath the caldera accommodate the inflation and deflation. Eruptions appear to occur at a predictable level of inflation; hence, it should be possible to time deployments of additional cabled and autonomous instrumentation to further enhance observations of the next eruption.

INTRODUCTION

There is a long history of supporting volcano observatories on land, where studies are motivated by the dual goals of mitigating the risks of eruptions and improving our scientific understanding of the role volcanoes play in transferring material and heat from the mantle and in forming Earth’s crust. Investigations of volcanoes combine discrete studies to characterize their structures and past eruptive histories with ongoing monitoring of ground deformation, seismicity,

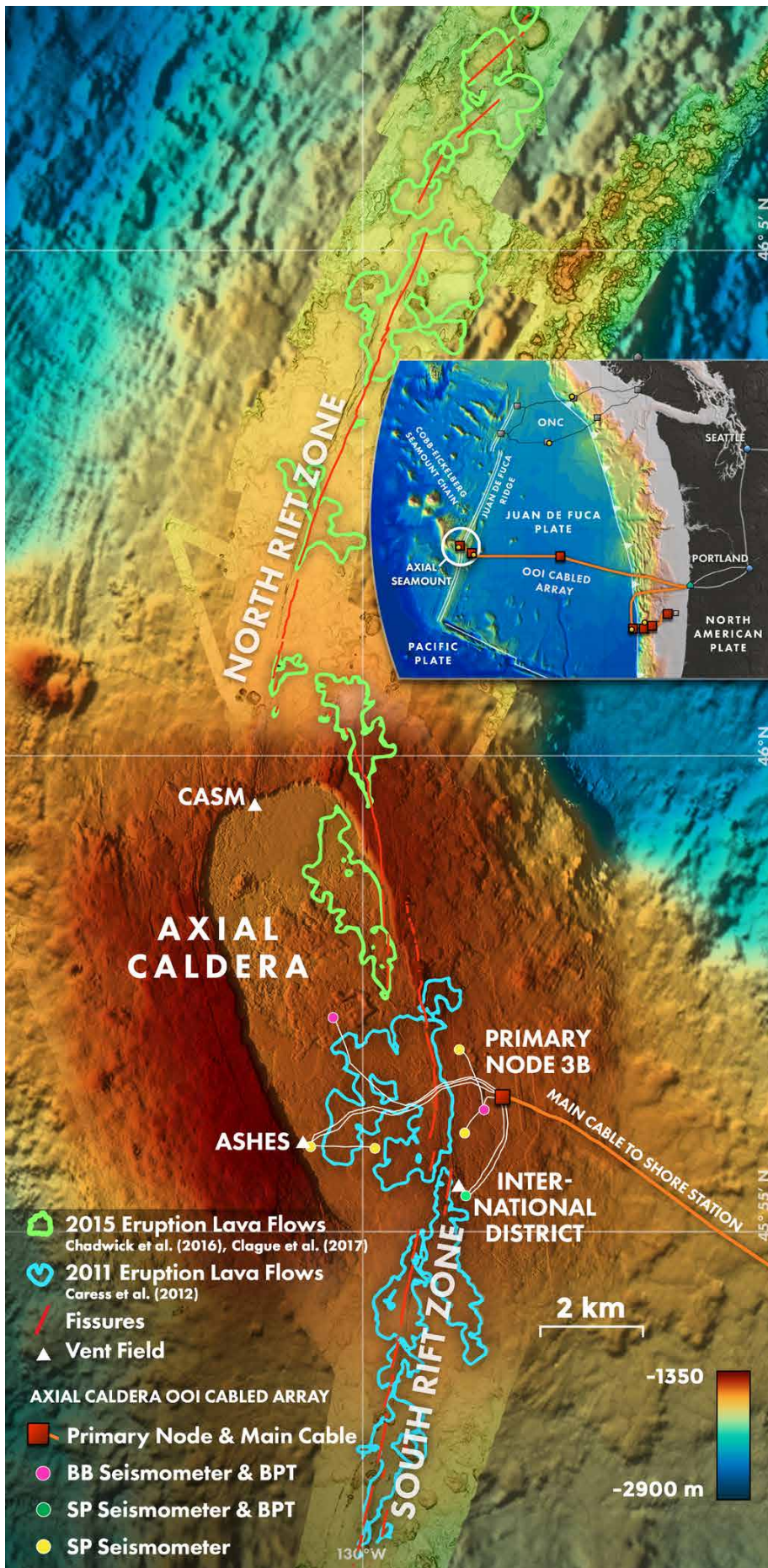
and the emissions of gas and geothermal fluids. Most volcanoes erupt infrequently and irregularly, and monitoring requires a commitment to long-term observations to characterize baseline behavior, detect early precursors of unrest, and record periods of activity.

In the ocean, studies of deepwater volcanoes are motivated by scientific goals. Volcanism at oceanic spreading centers replaces ~60% of the Earth’s surface on timescales of ~100 million years. Understanding this process requires observations of diking-eruptive events

and the “quantum events of upper oceanic crustal accretion” (Delaney et al., 1998). Hydrothermal systems on submarine volcanoes transport heat and chemicals into the ocean and feed chemosynthetic biological communities in a setting that may replicate the environment in which life first evolved on Earth and potentially elsewhere (Martin et al., 2008). Volcanic eruptions can reinvigorate existing hydrothermal vent fields and lead to the formation of event plumes, giant pulses of hydrothermal fluid that rise high in the water column from short-lived sources (Baker et al., 1999). Event plumes may flush out microorganisms from a subsurface biosphere that is otherwise hard to sample (Summit and Baross, 1998). Rapid response cruises have been organized to study submarine eruptions detected remotely by their seismicity (Duennebier et al., 1997; Cowen et al., 2004). However, because the timescales for diking, the onset of eruptions, and the formation of event plumes are hours to days, expeditions that arrive on site after a week or more are limited to observing the aftermath of these key processes.

These timing considerations motivated the installations of the Ocean Observatories Initiative (OOI) Cabled Array at Axial Seamount (Figure 1), an active volcano in the Northeast Pacific Ocean at the intersection of the Juan de Fuca Ridge oceanic spreading center and Cobb-Eickelberg seamount chain.

FACING PAGE. View of Axial Seamount from the south showing additional sensors that could be usefully added prior to the next eruption. Bathymetry from Clague et al. (2017). Lava flow outlines and Ocean Observatories Initiative Cabled Array geophysical instrumentation are as for Figure 1. Created by the University of Washington Center for Environmental Visualization



Axial Seamount rises ~1 km above the surrounding seafloor, and its summit is characterized by an elongated 8 km × 3 km caldera that hosts three high-temperature hydrothermal vent fields. Extensional rifts on the north and south flanks form segments of the Juan de Fuca Ridge that overlap in the caldera (Embley et al., 1990). The summit is underlain by an extensive and well-imaged magma body at 1–2 km depth that extends well beyond the northern and southern limits of the caldera (West et al., 2001; Arnulf et al., 2014).

The OOI Cabled Array at Axial Seamount is the most advanced underwater volcano observatory in the world (Kelley et al., 2014), and its siting benefits from over 30 years of expeditionary studies and sustained efforts to support near-continuous geophysical monitoring. During its first year of operation in 2015, the Cabled Array captured an eruption of the volcano in real time, adding to the records of two prior eruptions that were detected in 1998 and 2011.

In this paper, we review the geophysical observations of the three eruptions, each of which was recorded by a different configuration of sensors. Over its lifetime, the OOI Cabled Array will likely record more eruptions; the geodetic observations to date imply that eruptions will be predictable on timescales of one to a few years. With this in mind, we conclude by discussing how the observatory might be enhanced prior to the next eruption.

FIGURE 1. Bathymetric chart of Axial Seamount showing the configuration of geophysical instrumentation on the Ocean Observatories (OOI) Cabled Array and the location of fissures and lava flows associated with the 2011 (Caress et al., 2012) and 2015 (Chadwick et al., 2016; Clague et al., 2017) eruptions. The inset figure shows the location of Axial Seamount in the Northeast Pacific Ocean, the configuration of the OOI Cabled Array, and six hydrophones on the OOI and Ocean Networks Canada (ONC) cabled observatories (yellow circles) used to locate hydroacoustic events on April 24, 2011 (Figure 4c). Modified from Manalang and Delaney (2016), created by the University of Washington Center for Environmental Visualization

OBSERVATIONS PRIOR TO THE 1998 ERUPTION

Axial Seamount was first mapped with multibeam bathymetry and side-scan sonar systems in the early 1980s, and submersible-based studies of seafloor geology and hydrothermal venting commenced at the summit in 1983 (Chase et al., 1985; Butterfield et al., 1990). Sustained geophysical monitoring of Axial Seamount started in 1987 with the deployment of a bottom pressure recorder (BPR) near the center of the summit caldera (Fox, 1990). One or more BPRs were recovered and redeployed each summer. In 1996, these instruments were incorporated into the NOAA New Millennium Observatory (NeMO), a precursor to the OOI Cabled Array, that sought to obtain time-series observations of the interactions between volcanic activity and hydrothermal venting (Hammond et al., 2015).

The seismic networks on land in the Pacific Northwest are not sensitive enough to monitor volcanism on the Juan de Fuca Ridge, but because seismic signals propagate efficiently in the ocean sound channel, regional hydroacoustic monitoring provides an effective means for monitoring ocean spreading centers. In late 1991, NOAA was provided access to the US Navy Sound Surveillance System (SOSUS), a network of multiple element hydrophone arrays, for the purpose of monitoring the Juan de Fuca and Gorda Ridges for seismicity (Fox et al., 1994; Dziak et al., 2011); in 1993, the analysis became near-real time.

There was evidence from a short eight-day deployment of three ocean bottom seismometers (OBSs) in 1985 that Axial Seamount was seismically quite active (Jacobson et al., 1987), and from the onset of SOSUS monitoring in 1991, the rates of seismicity were clearly increasing. Over six years prior to the 1998 eruption, the SOSUS system, which had a detection threshold of magnitude ~ 2.5 (Fox et al., 1994; Dziak et al., 2011), recorded ~ 800 earthquakes concentrated in swarms (Dziak and Fox, 1999a; Figure 2b). A two-month

microearthquake survey with three OBSs in 1994 confirmed that seismicity rates were high (Tolstoy et al., 2002), and 400 earthquakes were located in the southern part of the caldera (Figure 3a).

1998 ERUPTION

The 1998 eruption at Axial Seamount started on January 25, and over 11 days SOSUS detected more than 8,000 earthquakes. Seismicity commenced at the summit and then, during the first two days, epicenters traced the southward propagation of a dike for ~ 50 km at a velocity of ~ 0.9 m s^{-1} for the first ~ 20 km and then at ~ 0.2 m s^{-1} (Figure 4a). Seismicity continued at the summit and southern end of the south rift for about a week after the migration ceased (Dziak and Fox, 1999b).

The BPR at the center of the caldera recorded a few centimeters of uplift starting 2.2 hours after seismicity began (Chadwick et al., 2013) followed by the onset of deflation 1.1 hours later. Over 3.2 m of deflation took place over six days, with most of it occurring in the

first two days as the dike propagated (Fox, 1999). A second BPR in the southeast caldera was caught in a lava flow very shortly after the onset of deflation at the central caldera (Fox et al., 2001). From these observations it was inferred that the dike took about three hours to propagate from the magma chamber to the seafloor (Fox, 1999; Chadwick et al., 2013).

Two five-element temperature moorings, extending 115 m above the seafloor, detected temperature anomalies within hours that peaked at 0.6°C and declined over two weeks (Baker et al., 1999). A response cruise that arrived on site 18 days after the eruption onset did not find an event plume over the caldera but found event-plume-like chemistry in a plume off-axis to the southwest. This led to speculation that the event plume discharge may have been sheared by strong currents (Lupton et al., 1999).

Differences between pre- and post-eruption bathymetry, coupled with side-scan data and seafloor observations, show that lava flows extended from the southeast caldera about 11 km down the

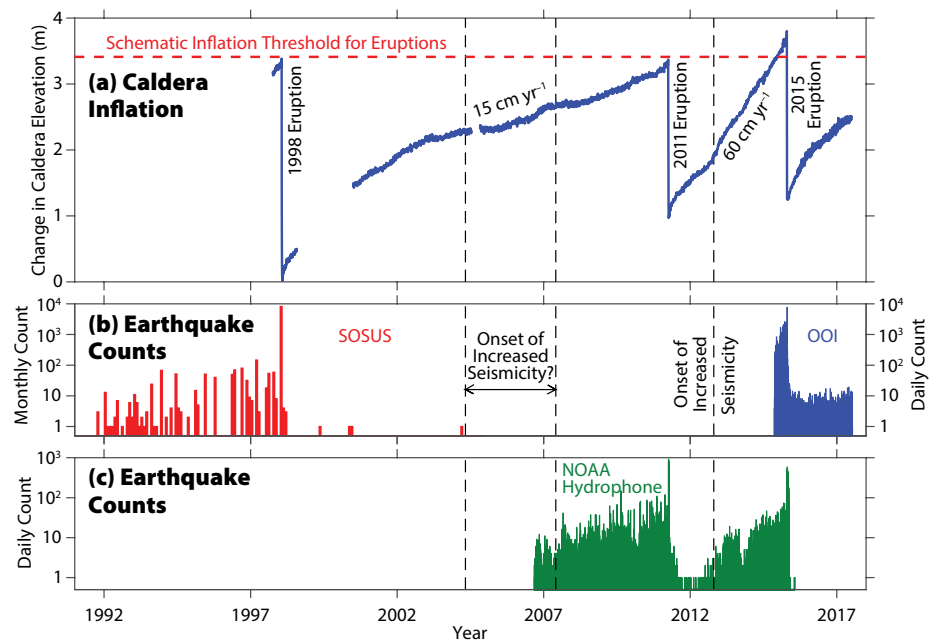


FIGURE 2. Long-term record of volcano inflation and deflation and earthquake counts at Axial Seamount. (a) Relative elevation at the center of the caldera (blue line) measured by combining data from continuously recording bottom pressure recorders with campaign-style calibration measurements from a mobile pressure recorder (modified from Nooner and Chadwick, 2016). (b–c) Histograms of earthquake counts plotted on logarithmic scales showing earthquakes detected per month by SOSUS (recreated from Dziak and Fox, 1999a), autonomous ocean bottom hydrophones (Caplan-Auerbach et al., 2017), and the OOI Cabled Array seismic network (Wilcock et al., 2016).

south rift (Embley et al., 1999; Chadwick et al., 2013). Interestingly, there is no evidence for an eruption at the southern end of the dike. The lava flow volume was estimated at $31 \times 10^6 \text{ m}^3$ and the volume of deflation at $207 \times 10^6 \text{ m}^3$, indicating that most of the magma removed from the summit reservoir was intrusive (Chadwick et al., 1999, 2013).

Following the 1998 eruption, seismicity at Axial Seamount declined dramatically (Dziak and Fox, 1999a), and over the next decade, SOSUS detected fewer than 10 earthquakes on the volcano. Starting two weeks after the 1998 eruption, three deployments of between four and 10 OBSs and ocean bottom hydrophones (OBHs) monitored microseismicity for 15 months

(Sohn et al., 2004). Only 140 microearthquakes were detected, an earthquake rate that is $\sim 5\%$ of that observed with a smaller network four years prior to the eruption (Tolstoy et al., 2002).

2011 ERUPTIVE CYCLE

Immediately following the 1998 eruption, the bottom pressure observations document a period of rapid re-inflation that is attributed either to recharge from secondary magma bodies or to poroelastic and viscoelastic re-equilibration following a sudden drop in pressure in the magma chamber (Nooner and Chadwick, 2009). After a two-year hiatus, bottom pressure observations resumed in 2000 with the addition of regular surveys using a mobile pressure recorder carried by a remotely operated vehicle. These surveys were designed to measure the difference in elevation between a set of benchmarks in and near the caldera and a reference benchmark on the volcano's flank (Chadwick et al., 2006). The resulting time series of calibrated bottom pressure records (Figure 2a) show an average inflation rate of $\sim 15 \text{ cm yr}^{-1}$ from 2000 to 2010 (Chadwick et al., 2012).

In the mid-2000s the SOSUS system became less reliable, and in 2008 the stations most useful for monitoring Axial Seamount went offline permanently. To continue the long-term observations, up to four autonomous NOAA OBHs were continuously operated in the caldera starting in 2006 (Dziak et al., 2012). The data show that the rates of microseismicity increased progressively over the five years of observations leading up to the 2011 eruption (Figure 2c).

Data from the autonomous hydrophones, however, were not available in real time, so in the absence of SOSUS monitoring, the 2011 eruption was not detected until new lava flows were discovered on the seafloor in July 2011 (Caress et al., 2012). The chronology of the eruption on April 6 was subsequently inferred from autonomous BPRs and OBHs (Chadwick et al., 2012; Dziak et al., 2012). There were several short-term precursors.

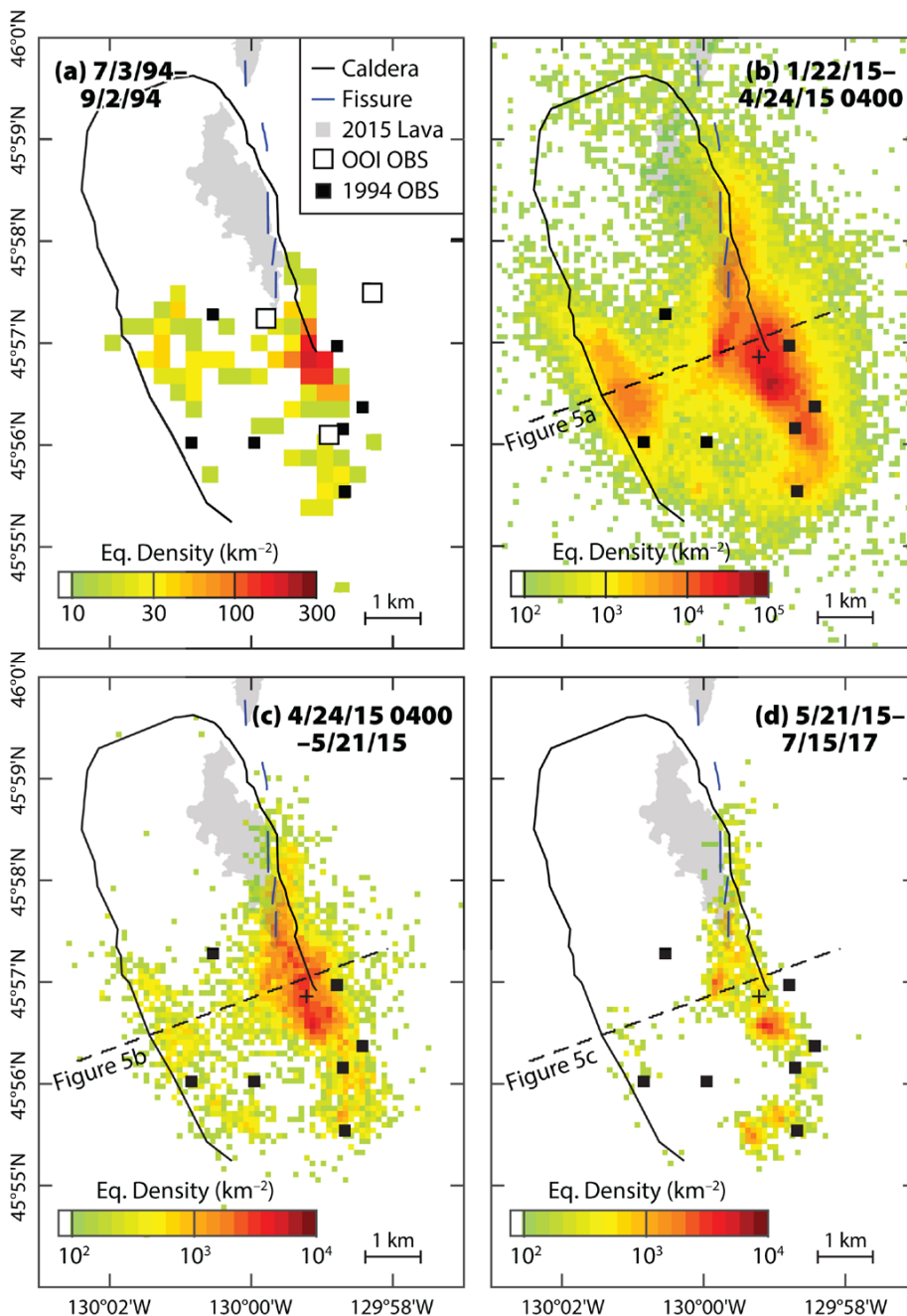


FIGURE 3. Maps showing the density of earthquake epicenters for (a) two months in 1994 (Tolstoy et al., 2002), and for the OOI Cabled Array seismic network for (b) the three months immediately prior to the 2015 eruption, (c) the 27-day duration of the 2015 eruption, ending when explosions ceased and the volcano started to re-inflate, and (d) the first 14 months of re-inflation. Note that the color scale for earthquake density is logarithmic, with threshold and color scales differing between plots.

For a few months leading up to the eruption, the rate of inflation steadily increased. Bursts of volcanic tremor, likely linked to subsurface magma movements, commenced several days beforehand. About eight hours before the eruption, the amplitude of short-term noise on the pressure recorders doubled.

The 2011 eruption itself shows many similarities to the 1998 eruption (Chadwick et al., 2013). The onset of seismicity occurred 2.6 hours before the eruption started, and acoustic amplitudes then increased rapidly, peaking 0.5 hours before the eruption, coincident with 7 cm of dike-induced uplift in the central caldera. The total deflation in the center of the caldera for the 2011 eruption was about 2.4 m, less than in 1998, but the duration of deflation and the time for acoustic amplitudes to decay were similar to those of the earlier eruption.

Because one of the three OBHs deployed at the time of the eruption was trapped in 2011 lava, there are no earthquake locations to track the propagation of the dike (Dziak et al., 2012). Fresh lava flows were found extending from the center of the caldera to about 10 km south. About 30 km south of the caldera, bathymetric difference maps delineated a 5 km-long pillow ridge with a maximum thickness of 140 m that postdates the 1998 eruption and is reasonably inferred to be part of the 2011 eruption (Caress et al., 2012). The northern eruption occupied many of the same eruptive fissures as the 1998 eruption and has a similar footprint and volume ($33 \times 10^6 \text{ m}^3$), while the more southern lava flow has a volume of $66 \times 10^6 \text{ m}^3$. The total volume of deflation estimated using a point source elastic deformation model is $147 \times 10^6 \text{ m}^3$, of which about two-thirds was erupted (Chadwick et al., 2012). Thus, while smaller in total volume than the 1998 eruption, the volume of extruded lavas was much higher in 2011.

OOI CABLED ARRAY AND 2015 ERUPTION

Shortly after the 2011 eruption, Chadwick et al. (2012) postulated that eruptions of Axial Seamount occur at a threshold level of inflation and stated that if the volcano re-inflated in the same pattern as observed after the 1998 eruption, it could be ready to erupt again in 2018. The initial pattern of re-inflation at Axial was similar to the prior eruption, but by 2013 it was clear that the inflation was continuing at a higher rate of $\sim 60 \text{ cm yr}^{-1}$ (Figure 2a) due to increased magma supply. This observation led in September 2014 to a revised forecast that the volcano would erupt in 2015 (Chadwick and Nooner, 2014). The earthquake rate measured by the NOAA OBHs also started to increase in fall 2012 (Caplan-Auerbach et al., 2017) and then increased up to the time of the 2015 eruption more quickly than observed prior to the 2011 eruption (Figure 2c), consistent with the higher rate of re-inflation. The earthquake rates just before the eruptions were similar in 2011 and 2015.

Installation of the OOI Cabled Array at Axial Seamount was completed late in the summer of 2014, with the observatory coming on line that fall (Kelley et al., 2014). The system

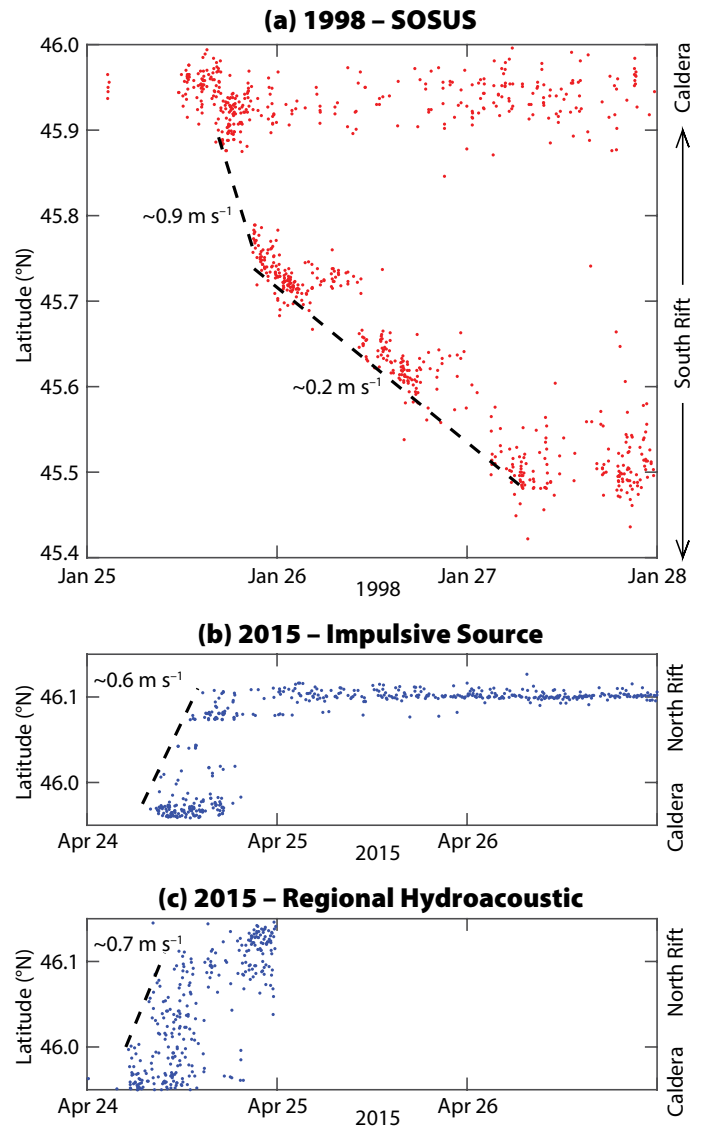


FIGURE 4. Migration of earthquakes and impulsive seafloor signals for the 1998 and 2015 eruptions. (a) Latitude of SOSUS epicenters for the first three days of the 1998 eruption (Dziak and Fox, 1999b). (b) Latitude of eruption-related seafloor impulsive signals determined with the OOI Cabled Array caldera seismic network for the 2015 eruption. (c) Latitude of earthquakes and seafloor impulsive signals for the first day of the 2015 eruption determined with hydrophones from the OOI and ONC cabled observatories (see Figure 1 inset).

incorporates geophysical instrumentation on both the Cascadia margin (Tréhu et al., 2018, in this issue) and Axial Seamount. At the summit of Axial Seamount, the footprint of the observatory (Figure 1) spans the southern half of the caldera where the 1998 and 2011 eruptions initiated. The seismic component of the observatory includes seven three-component seismic stations; five are short period instruments that are attached to leveled triangular baseplates (Figure S1a), and two are broadband instruments in spherical housings that are co-located with hydrophones (Figure S1b). The broadband stations sit on basaltic seafloor and are surrounded by sandbags to improve coupling. When the observatory was installed, three of the seismic

stations were co-located with geodetic sensors that measure bottom pressure and seafloor tilt (Figures 1 and S1c). These instruments are complemented by autonomous BPRs at several other sites. A fourth cabled bottom pressure and tilt instrument was added at the ASHES (Axial Seamount Hydrothermal Emission Study) vent field in summer 2017.

The rates of seismicity were already high when the OOI Cabled Array came online in November 2014, and the number of earthquakes detected by this system increased from a few hundred per day to about two thousand per day a month before the eruption (Figure 2b; Wilcock et al., 2016). The presence of a local seismic network on top of the volcano has allowed over 100,000 earthquakes to be located. Their distributions before, during, and after the eruption (Figure 3b–d) are similar to one another and to the distribution observed in 1994 (Figure 3a), although after the eruption a larger proportion of the earthquakes occur at the southern end of the caldera and a smaller proportion on the west wall. The majority of the earthquakes are concentrated below the east wall of the caldera, with the highest density near the centroid of inflation determined from the bottom pressure data (Nooner and Chadwick, 2016). There is also a high density of earthquakes near the west wall and beneath the southern end of the caldera. Cumulatively, these earthquakes define an outward-dipping ring fault

(Figure 5) that accommodates some of the uplift of the caldera prior to an eruption and then, by reversing the direction of fault motion, some of the subsidence during an eruption (Wilcock et al., 2016).

The rate of seismicity decreased slightly two weeks before the eruption, but the only seismic precursor was tremor starting six hours beforehand, a markedly shorter warning than seen for the 2011 eruption. The onset of increased seismicity on April 24 preceded peak seismic amplitudes and the onset of deflation by about two hours. The total amount of deflation was similar to 2011, but the volcano deflated more quickly (Nooner and Chadwick, 2016), with the majority of earthquakes occurring during the ~10-hour seismic “crisis.”

One unexpected observation from this eruption was the detection of tens of thousands of impulsive water-borne signals (Wilcock et al., 2016; Tolstoy et al., 2018, in this issue) that started within hours of the seismic crisis and continued for nearly a month, ceasing when the bottom pressure data showed that the volcano started to re-inflate and the seismicity rates reached very low levels. The mechanism for these signals is uncertain, but they are clearly related to lava erupting on the seafloor. The impulsive signals can be located by modeling the times of the water column reverberations. They can be spatially linked to lava flows, and the majority were located ~10–15 km along the north rift where thick pillow

flows were subsequently discovered. The OOI hydrophones at the summit of Axial Seamount also recorded diffuse events in the later stages of the eruption that were interpreted as possible explosive submarine ash eruptions (Caplan-Auerbach et al., 2017).

The earthquake locations show that early in the eruption, earthquakes migrated 2–3 km south from the north-east edge of the caldera before stalling near the northern limit of the two prior eruptions (Wilcock et al., 2016). The locations show no evidence of the dike propagating northward along the north rift. This is a result of the limited footprint of the seismic network, the high noise levels generated by local earthquakes, and shadowing from the axial magma chamber that extends well to the north of the caldera and would lie in the path of seismic waves traveling from earthquakes on the north rift.

There is evidence for northward dike propagation based on the onset time of the impulsive signals as a function of their latitude (Figure 4b). Using these data to get the dike propagation rate requires an untested assumption that the interval between the passage of the dike and the onset of impulsive signals is constant. A more robust estimate of the dike propagation speed can be obtained from regional hydroacoustic locations. In combination, the hydrophones on the OOI Cabled Array and the Ocean Networks Canada NEPTUNE cabled observatory

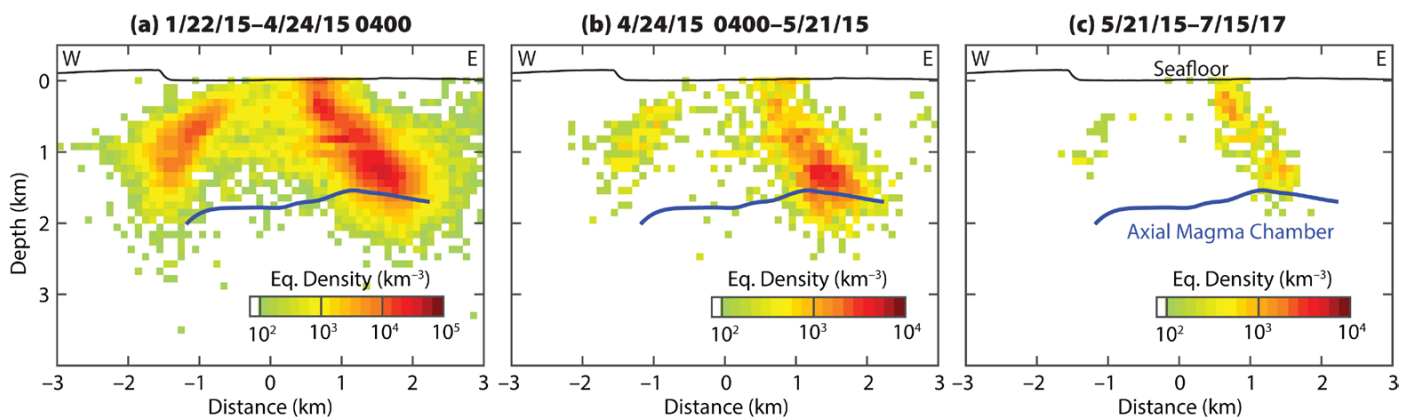


FIGURE 5. Vertical cross sections oriented WSW-ENE across the southern caldera (dashed lines in Figure 3b–d), showing the density of earthquake hypocenters lying within 0.5 km of the cross section for the same time intervals (a) before, (b) during, and (c) after the eruption as shown in Figure 3b–d.

provide a reasonable geometry for triangulating locations on Axial Seamount (Figure 1 inset). Hydroacoustic locations obtained for April 24 (Figure 4c) suggest that northward dike propagation started early in the seismic crisis, coincident with the onset of deflation, and that the dike propagated at $\sim 0.7 \text{ m s}^{-1}$, possibly slowing near its northern end, as was observed for the 1998 dike.

The larger number of bottom pressure measurement sites for the 2015 eruption from an array of 10 seafloor benchmarks permitted calculation of more complex source geometries than was possible for prior eruptions. The best fitting source was a steeply dipping prolate-spheroid, with a co-eruption decrease in volume of $2.88 \times 10^8 \text{ m}^3$ (Nooner and Chadwick, 2016). Just over half of that volume erupted onto the seafloor, mostly in the northern lava flows (Chadwick et al., 2016); the rest was inferred to have filled a 24 km-long, 2–3 m-wide dike. The large width is consistent with the rapid deflation observed (Nooner and Chadwick, 2016).

FUTURE OF VOLCANO MONITORING AT AXIAL

Volcano monitoring at Axial Seamount has contributed substantially to our understanding of submarine volcanism. Along with the East Pacific Rise at $9^{\circ}50'N$ (Tolstoy et al., 2006), it is one of only two sites on an oceanic spreading center where more than one eruption has been observed and the only site where geodetic and seismic observations have been obtained concurrently through an eruption. As of summer 2017, the volcano has recovered about half of the deflation that occurred during the 2015 eruption, with the rate of inflation declining from $\sim 1 \text{ m yr}^{-1}$ immediately after the eruption to $\sim 0.40 \text{ m yr}^{-1}$ recently. If the volcano continues to inflate at $\sim 0.40 \text{ m yr}^{-1}$, another eruption is expected in three years, but the inflation rate may vary. Interestingly, the volcano remains seismically quiet. Because the level of inflation has already exceeded that at which seismicity rates started to increase prior to

the 2015 eruption and is similar to that at which the seismicity rate was increasing prior to the 2011 eruption (Figure 2), we infer that the rate of seismicity will soon start to increase, providing another indicator of the time to the next eruption.

One lesson learned from monitoring seismicity at Axial Seamount is the importance of nested observations. The cabled seismometer and hydrophone

new opportunities for understanding the mechanics of submarine diking events by constraining the depth and style of faulting and measuring variations in the speed of propagation.

Another goal for the next eruption should be to enhance hydrothermal observations. At present, the Cabled Array incorporates a variety of instrumentation in the ASHES and International District

“ Along with the East Pacific Rise at $9^{\circ}50'N$, [Axial Seamount] is one of only two sites on an oceanic spreading center where more than one eruption has been observed and the only site where geodetic and seismic observations have been obtained concurrently through an eruption. ”

network at the summit has provided an unprecedented data set that is being mined to understand the dynamics of a submarine caldera as well as the source of eruption-generated sounds. However, the network did not detect earthquakes associated with the northward propagation of the dike that fed the most voluminous lava flows. Regional hydroacoustic monitoring with the OOI and Ocean Networks Canada hydrophones constrained the rate of propagation for the 2015 dike (Figure 4c), but distant hydroacoustic observations cannot easily distinguish between shallow earthquakes and impulsive seafloor events, and they provide only a weak constraint on source depth (Dziak and Fox, 1999b). For the next eruption, the cabled seismic and regional hydroacoustic observations should be complemented by temporary deployments of OBSs to cover the northern part of the caldera and upper portions of north and south rifts and the moored hydrophones that encircle the seamount (title page and Figure S2). This would provide

vent fields (Figure 1), but no significant perturbations were observed in these hydrothermal vents for the 2015 eruption because the dike and the lava flows were located well to the north of these fields. Because it is unknown whether the next dike will be emplaced on the north or south rift, deploying sensors in the CASM (Canadian American Seamount) vent field at the north end of the caldera (Figures 1 and S2 and title page) would ensure that at least one monitored vent field is close to the next dike.

Although numerous event plumes have been observed after formation either by response cruises or serendipity, their formation mechanism remains unclear and has been alternatively attributed to cooling lava flows (Palmer and Ernst, 1998), cooling dikes (Lowell and Germanovich, 1995), or the release of mature hydrothermal fluids already present in the crust (Cann and Strens, 1989). One approach to studying both steady-state and event plumes would be to build upon water column temperature observations from the

1998 eruption (Baker et al., 1999) and install moorings in and near the caldera (title page and Figure S2). Alternatively, ocean gliders could be deployed to survey the hydrothermal plumes as is done at many of the other OOI observatory sites.

Manalang and Delaney (2016) explore the feasibility of adding a resident autonomous underwater vehicle at Axial Seamount. It would dock to the Cabled Array to recharge batteries and download data, and utilize a network of acoustic transponders to navigate and communicate while executing missions (title page and Figure S2). If event plumes form above thick lava flows, such as those found down the rifts in 2011 and 2015, mobile platforms may be the most practical means of observing the eruption in progress and event plumes during their formation. An acoustic transponder network could also complement an expanded set of bottom pressure measurements by enabling horizontal geodesy between pairs of transponders that would further constrain models of caldera inflation and measure the extension that occurs when dikes are emplaced.

The 2015 eruption at Axial Seamount was the first to be recorded by an in situ cabled observatory, and Axial is now the best-monitored submarine volcano on Earth. More was learned about Axial Seamount's internal plumbing in 2015 than in the previous eruptions because of the many multidisciplinary observations enabled by the cabled network. The 2015 eruption also showed where knowledge gaps exist and where any new monitoring assets might be deployed to learn even more in the future. Ultimately, the real-time data provided through OOI will enable better preparation for future eruptions both on an annual timescale by deployment of additional autonomous sensors as the volcano nears its critical state, and on an hourly timescale through deployment and rapid sampling of all available Cabled Array assets as seismic and geodetic signals indicate an eruption is imminent or underway. 

SUPPLEMENTARY MATERIALS

Supplementary Figures S1 and S2 are available online at <https://doi.org/10.5670/oceanog.2018.117>.

REFERENCES

- Arnulf, A.F., A.J. Harding, G.M. Kent, S.M. Carbotte, J.P. Canales, and M. Nedimovic. 2014. Anatomy of an active submarine volcano. *Geology* 42(8):655–658, <https://doi.org/10.1130/G35629.1>.
- Baker, E.T., C.G. Fox, and J.P. Cowen. 1999. In situ observations of the onset of hydrothermal discharge during the 1998 submarine eruption of Axial Volcano, Juan de Fuca Ridge. *Geophysical Research Letters* 26(23):3,445–3,448, <https://doi.org/10.1029/1999GL002331>.
- Butterfield, D.A., G.J. Massoth, R.E. McDuff, J.E. Lupton, and M.D. Lilley. 1990. Geochemistry of hydrothermal fluids from Axial Seamount hydrothermal emissions study vent field, Juan de Fuca Ridge: Subseafloor boiling and subsequent fluid-rock interaction. *Journal of Geophysical Research* 95(B8):12,895–12,921, <https://doi.org/10.1029/JB095iB08p12895>.
- Cann, J.R., and M.R. Strens. 1989. Modeling periodic megaplume emission by black smoker systems. *Journal of Geophysical Research* 94(B9):12,227–12,237, <https://doi.org/10.1029/JB094iB09p12227>.
- Caplan-Auerbach, J., R.P. Dziak, J. Haxel, D.R. Bohnenstiehl, and C. Garcia. 2017. Explosive processes during the 2015 eruption of Axial Seamount, as recorded by seafloor hydrophones. *Geochemistry, Geophysics, Geosystems* 18(4):1,761–1,774, <https://doi.org/10.1002/2016GC006734>.
- Caress, D.W., D.A. Clague, J.B. Paduan, J.F. Martin, B.M. Dreyer, W.W. Chadwick Jr., A. Denny, and D.S. Kelley. 2012. Repeat bathymetric surveys at 1-metre resolution of lava flows erupted at Axial Seamount in April 2011. *Nature Geoscience* 5(7):483–488, <https://doi.org/10.1038/ngeo1496>.
- Chadwick, W.W., Jr., D.A. Clague, R.W. Embley, M.R. Perfit, D.A. Butterfield, D.W. Caress, J.B. Paduan, J.F. Martin, P. Sasnett, S.G. Merle, and A.M. Bobbitt. 2013. The 1998 eruption of Axial Seamount: New insights on submarine lava flow emplacement from high-resolution mapping. *Geochemistry, Geophysics, Geosystems* 14(10):3,939–3,968, <https://doi.org/10.1002/ggge.20202>.
- Chadwick, W.W., Jr., R.W. Embley, H.B. Milburn, C. Meinig, and M. Stapp. 1999. Evidence for deformation associated with the 1998 eruption of Axial Volcano, Juan de Fuca Ridge, from acoustic extensometer measurements. *Geophysical Research Letters* 26(23):3,441–3,444, <https://doi.org/10.1029/1999GL900498>.
- Chadwick, W.W., Jr., and S.L. Nooner. 2014. Slide from a talk at the Monterey Bay Aquarium Research Institute (MBARI). *Blog to Chronicle Eruption Forecasts at Axial Seamount*, https://www.pmel.noaa.gov/eoi/axial_blog.html.
- Chadwick, W.W. Jr., S.L. Nooner, D.A. Butterfield, and M.D. Lilley. 2012. Seafloor deformation and forecasts of the April 2011 eruption at Axial Seamount. *Nature Geoscience* 5(7):474–477, <https://doi.org/10.1038/ngeo1464>.
- Chadwick, W.W., Jr., S.L. Nooner, M.A. Zumberge, R.W. Embley, and C.G. Fox. 2006. Vertical deformation monitoring at Axial Seamount since its 1998 eruption using deep-sea pressure sensors. *Journal of Volcanology and Geothermal Research* 150(1):313–327, <https://doi.org/10.1016/j.jvolgeores.2005.07.006>.
- Chadwick, W.W., Jr., J.B. Paduan, D.A. Clague, B.M. Dreyer, S.G. Merle, A.M. Bobbitt, D.W. Caress, B.T. Philip, D.S. Kelley, and S.L. Nooner. 2016. Voluminous eruption from a zoned magma body after an increase in supply rate at Axial Seamount. *Geophysical Research Letters* 43(23):12,063–12,070, <https://doi.org/10.1002/2016GL071327>.
- Chase, R., J. Delaney, J. Karsten, H. Johnson, S. Juniper, J. Lupton, S. Scott, V. Tunnaciff, R. Hammond, and R. McDuff. 1985. Hydrothermal vents on an axis seamount of the Juan de Fuca ridge. *Nature* 317(5999):212–214, <https://doi.org/10.1038/313212a0>.
- Clague, D.A., J.B. Paduan, D.W. Caress, W.W. Chadwick Jr., M. Le Saout, B.M. Dreyer, and R.A. Portner. 2017. High-resolution AUV mapping and targeted ROV observations of three historical lava flows at Axial Seamount. *Oceanography* 30(4), <https://doi.org/10.5670/oceanog.2017.426>.
- Cowen, J.P., E.T. Baker, and R.W. Embley. 2004. Detection of and response to mid-ocean ridge magmatic events: Implications for the subsurface biosphere. Pp. 227–243 in *The Subseafloor Biosphere at Mid-Ocean Ridges*. W.S.D. Wilcock, E.F. DeLong, D.S. Kelley, J.A. Baross, and S.C. Cary, eds, Geophysical Monograph Series, vol. 144, American Geophysical Union, Washington, DC.
- Delaney, J.R., D.S. Kelley, M.D. Lilley, D.A. Butterfield, J.A. Baross, W.S.D. Wilcock, R.W. Embley, and M. Summit. 1998. The quantum event of oceanic crustal accretion: Impacts of diking at mid-ocean ridges. *Science* 281(5374):222–230, <https://doi.org/10.1126/science.281.5374.222>.
- Duennebieber, F.K., N.C. Becker, J. Caplan-Auerbach, D.A. Clague, J. Cowen, M. Cremer, M. Garcia, F. Goff, A. Malahoff, G.M. McMurtry, and others. 1997. Researchers rapidly respond to submarine activity at Loihi Volcano, Hawaii. *Eos, Transactions American Geophysical Union* 78(22):229, <https://doi.org/10.1029/97EO00150>.
- Dziak, R.P., and C.G. Fox. 1999a. Long-term seismicity and ground deformation at Axial Volcano, Juan de Fuca Ridge. *Geophysical Research Letters* 26(24):3,641–3,644, <https://doi.org/10.1029/1999GL002326>.
- Dziak, R.P., and C.G. Fox. 1999b. The January 1998 earthquake swarm at Axial Volcano, Juan de Fuca Ridge: Hydroacoustic evidence of seafloor volcanic activity. *Geophysical Research Letters* 26(23):3,429–3,432, <https://doi.org/10.1029/1999GL002332>.
- Dziak, R.P., S.R. Hammond, and C.G. Fox. 2011. A 20-year hydroacoustic time series of seismic and volcanic events in the Northeast Pacific Ocean. *Oceanography* 24(3):280–293, <https://doi.org/10.5670/oceanog.2011.79>.
- Dziak, R.P., J.H. Haxel, D.R. Bohnenstiehl, W.W. Chadwick Jr., S.L. Nooner, M.J. Fowler, H. Matsumoto, and D.A. Butterfield. 2012. Seismic precursors and magma ascent before the April 2011 eruption at Axial Seamount. *Nature Geoscience* 5(7):478–482, <https://doi.org/10.1038/ngeo1490>.
- Embley, R.W., K.M. Murphy, and C.G. Fox. 1990. High-resolution studies of the summit of Axial Volcano. *Journal of Geophysical Research* 95(8):12,785–12,812, <https://doi.org/10.1029/JB095iB08p12785>.
- Embley, R.W., W.W. Chadwick Jr., D. Clague, and D. Stakes. 1999. 1998 eruption of Axial Volcano: Multibeam anomalies and sea-floor observations. *Geophysical Research Letters* 26(23):3,425–3,428, <https://doi.org/10.1029/1999GL002328>.

- Fox, C.G. 1990. Evidence of active ground deformation on the mid-ocean ridge: Axial Seamount, Juan de Fuca Ridge, April–June 1988. *Journal of Geophysical Research* 95(B8):12,813–12,822, <https://doi.org/10.1029/JB095iB08p12813>.
- Fox, C.G. 1999. In situ ground deformation measurements from the summit of Axial Volcano during the 1998 volcanic episode. *Geophysical Research Letters* 26(23):3,437–3,440.
- Fox, C.G., W.W. Chadwick Jr., and R.W. Embley. 2001. Direct observation of a submarine volcanic eruption from a sea-floor instrument caught in a lava flow. *Nature* 412(6848):727–729, <https://doi.org/10.1038/35089066>.
- Fox, C.G., R.P. Dziak, H. Matsumoto, and A.E. Schreiner. 1994. Potential for monitoring low-level seismicity on the Juan de Fuca Ridge using military hydrophone arrays. *Marine Technology Society Journal* 27(4):22–30.
- Hammond, S.R., R.W. Embley, and E.T. Baker. 2015. The NOAA vents program 1983 to 2013: Thirty years of ocean exploration and research. *Oceanography* 28(1):160–173, <https://doi.org/10.5670/oceanog.2015.17>.
- Jacobson, R.S., L.D. Bibee, R.W. Embley, and S.R. Hammond. 1987. A microseismicity survey of Axial Seamount, Juan de Fuca Ridge. *Bulletin of the Seismological Society of America* 77(1):160–172.
- Kelley, D.S., J.R. Delaney, and S.K. Juniper. 2014. Establishing a new era of submarine volcanic observatories: Cabling Axial Seamount and the Endeavour Segment of the Juan de Fuca Ridge. *Marine Geology* 352:426–450, <https://doi.org/10.1016/j.margeo.2014.03.010>.
- Lowell, R., and L. Germanovich. 1995. Dike injection and the formation of megaplumes at ocean ridges. *Science* 267(5205):1804, <https://doi.org/10.1126/science.267.5205.1804>.
- Lupton, J., E. Baker, R. Embley, R. Greene, and L. Evans. 1999. Anomalous helium and heat signatures associated with the 1998 Axial Volcano Event, Juan de Fuca Ridge. *Geophysical Research Letters* 26(23):3,449–3,452, <https://doi.org/10.1029/1999GL002330>.
- Manalang, D., and J.R. Delaney. 2016. Axial seamount—restless, wired and occupied: A conceptual overview of resident AUV operations and technologies. Paper presented at *OCEANS 2016 MTS/IEEE*, September 19–23, 2016, Monterey, CA, <https://doi.org/10.1109/OCEANS.2016.7761305>.
- Martin, W., J. Baross, D. Kelley, and M.J. Russell. 2008. Hydrothermal vents and the origin of life. *Nature Reviews Microbiology* 6:805–814, <https://doi.org/10.1038/nrmicro1991>.
- Nooner, S.L., and W.W. Chadwick Jr. 2009. Volcanic inflation measured in the caldera of Axial Seamount: Implications for magma supply and future eruptions. *Geochemistry, Geophysics, Geosystems* 10(2), Q02002, <https://doi.org/10.1029/2008GC002315>.
- Nooner, S.L., and W.W. Chadwick Jr. 2016. Inflation-predictable behavior and co-eruption deformation at Axial Seamount. *Science* 354(6318):1,399–1,403, <https://doi.org/10.1126/science.aah4666>.
- Palmer, M.R., and G.G.J. Ernst. 1998. Generation of hydrothermal megaplumes by cooling of pillow basalts at mid-ocean ridges. *Nature* 393(6686):643–647, <https://doi.org/10.1038/31397>.
- Sohn, R.A., A.H. Barclay, and S.C. Webb. 2004. Microearthquake patterns following the 1998 eruption of Axial Volcano, Juan de Fuca Ridge: Mechanical relaxation and thermal strain. *Journal of Geophysical Research* 109, B01101, <https://doi.org/10.1029/2003JB002499>.
- Summit, M., and J.A. Baross. 1998. Thermophilic sea-floor microorganisms from the 1996 North Gorda Ridge eruption. *Deep Sea Research Part II* 45(12):2,751–2,766, [https://doi.org/10.1016/S0967-0645\(98\)00092-7](https://doi.org/10.1016/S0967-0645(98)00092-7).
- Tolstoy, M., F.L. Vernon, J.A. Orcutt, and F.K. Wyatt. 2002. Breathing of the seafloor: Tidal correlations of seismicity at Axial Volcano. *Geology* 30(6):503–506, [https://doi.org/10.1130/0091-7613\(2002\)030<0503:BOTSTC>2.0.CO;2](https://doi.org/10.1130/0091-7613(2002)030<0503:BOTSTC>2.0.CO;2).
- Tolstoy, M., W.S.D. Wilcock, Y.J. Tan, and F. Waldhauser. 2018. A tale of two eruptions: How data from Axial Seamount led to a discovery on the East Pacific Rise. *Oceanography* 31(1):124–125, <https://doi.org/10.5670/oceanog.2018.118>.
- Tolstoy, T., J.P. Cowen, E.T. Baker, D.J. Fornari, K.H. Rubin, T.M. Shank, F. Waldhauser, D.R. Bohnenstiehl, D.W. Forsyth, R.C. Holmes, and others. 2006. A sea-floor spreading event captured by seismometers. *Science* 314(5807):1,920–1,922, <https://doi.org/10.1126/science.1133950>.
- Tréhu, A.M., W.S.D. Wilcock, R. Hilmo, P. Bodin, J. Connolly, E.C. Roland, and J. Braunmiller. 2018. The role of the Ocean Observatories Initiative in monitoring the offshore earthquake activity of the Cascadia subduction zone. *Oceanography* 31(1):104–113, <https://doi.org/10.5670/oceanog.2018.116>.
- West, M., W. Menke, M. Tolstoy, S. Webb, and R. Sohn. 2001. Magma storage beneath Axial Volcano on the Juan de Fuca mid-ocean ridge. *Nature* 413(6858):833–836, <https://doi.org/10.1038/35101581>.
- Wilcock, W.S.D., M. Tolstoy, F. Waldhauser, C. Garcia, Y.J. Tan, D.R. Bohnenstiehl, J. Caplan-Auerbach, R.P. Dziak, A.F. Arnulf, and M.E. Mann. 2016. Seismic constraints on caldera dynamics from the 2015 Axial Seamount eruption. *Science* 354(6318):1,395–1,399, <https://doi.org/10.1126/science.aah5563>.

ACKNOWLEDGMENTS

We thank John Delaney, Deborah Kelley, and the OOI Cabled Array team for their efforts to design, install, and operate the Cabled Array. This work was supported by the National Science Foundation under awards OCE-1536219, 1536320, 1546616, 1356216, 1635276, and 1357076. This paper is Pacific Marine Environmental Laboratory contribution number 4715.

AUTHORS

William S.D. Wilcock (wilcock@uw.edu) is Jerome M. Paros Endowed Chair in Sensor Networks, School of Oceanography, University of Washington, Seattle, WA, USA. **Robert P. Dziak** is Acoustics Program Manager, National Oceanic and Atmospheric Administration/Pacific Marine Environmental Laboratory (NOAA/PMEL), Newport, OR, USA. **Maya Tolstoy** is Professor, Lamont-Doherty Earth Observatory of Columbia University, Palisades, NY, USA. **William W. Chadwick Jr.** is Professor, Oregon State University/Cooperative Institute for Marine Resources Studies, and NOAA/PMEL, Newport, Oregon, USA. **Scott L. Nooner** is Associate Professor, University of North Carolina Wilmington, Wilmington, NC, USA. **DelWayne R. Bohnenstiehl** is Associate Professor, Department of Marine, Earth, and Atmospheric Sciences, North Carolina State University, Raleigh, NC, USA. **Jacqueline Caplan-Auerbach** is Associate Professor, Geology Department, Western Washington University, Bellingham, WA, USA. **Felix Waldhauser** is Lamont Research Professor, Lamont-Doherty Earth Observatory of Columbia University, Palisades, NY, USA. **Adrien F. Arnulf** is Research Associate, Institute for Geophysics, Jackson School of Geosciences, University of Texas, Austin, TX, USA.

Christian Baillard is Research Associate, School of Oceanography, University of Washington, Seattle, WA, USA. **Tai-Kwan Lau** is Applied Mathematician, and **Joseph H. Haxel** is Assistant Professor, both at Oregon State University/Cooperative Institute for Marine Resources Studies, and NOAA/PMEL, Newport, Oregon, USA. **Yen Joe Tan** is a graduate student at Lamont-Doherty Earth Observatory of Columbia University, Palisades, NY, USA. **Charles Garcia** is a graduate student in the School of Oceanography, University of Washington, Seattle, WA, USA. **Samuel Levy** is a graduate student in the Department of Marine, Earth, and Atmospheric Sciences, North Carolina State University, Raleigh, NC, USA. **M. Everett Mann** is a graduate student in the Department of Earth and Atmospheric Sciences, Cornell University, Ithaca, NY, USA.

ARTICLE CITATION

Wilcock, W.S.D., R.P. Dziak, M. Tolstoy, W.W. Chadwick Jr., S.L. Nooner, D.R. Bohnenstiehl, J. Caplan-Auerbach, F. Waldhauser, A.F. Arnulf, C. Baillard, T.-K. Lau, J.H. Haxel, Y.J. Tan, C. Garcia, S. Levy, and M.E. Mann. 2018. The recent volcanic history of Axial Seamount: Geophysical insights into past eruption dynamics with an eye toward enhanced observations of future eruptions. *Oceanography* 31(1):114–123, <https://doi.org/10.5670/oceanog.2018.117>.